Cellulose (2022) 29:7649–7662
https://doi.org/10.1007/s10570-022-04719-y

ORIGINAL RESEARCH

The effect of ionic strength and pH on the dewatering rate of cellulose nanofibril dispersions

Andreas Fall · Marielle Henriksson · Anni Karppinen · Anne Opstad · Ellinor B. Heggset · Kristin Syverud

Received: 9 December 2021 / Accepted: 13 June 2022 / Published online: 20 July 2022

Abstract Cellulose nanofibrils, CNFs, show great potential in many application areas. One main aspect limiting the industrial use is the slow and energy demanding dewatering of CNF suspensions. Here we investigate the dewatering with a piston press process. Three different CNF grades were dewatered to solid contents between approx. 20 and 30%. The CNF grades varied in charge density (30, 106 and 604 µmol/g) and fibrillation degree. The chemical conditions were varied by changing salt concentration (NaCl) and pH and the dewatering rates were compared before and after these changes. For the original suspensions, a higher charge provides slower dewatering with the substantially slowest dewatering for the highest charged CNFs. However, by changing the conditions it dewatered as fast as the two lower charged CNFs, even though the salt/acid additions also improved the dewatering rate for these two CNFs. Finally, by tuning the conditions, fast dewatering could be obtained with only minor effect on film properties (strength and oxygen barrier) produced from redispersed dispersion. However, dewatering gives some reduction in viscosity of the redispersed dispersions. This may be a disadvantage if the CNF application is as e.g. rheology modifier or emulsion stabilizer.

Supplementary Information The online version contains supplementary material available at https://doi.org/10.1007/s10570-022-04719-y.

A. Fall · M. Henriksson
RISE Research Institutes of Sweden, Box 5604, 114 86 Stockholm, Sweden

A. Karppinen · A. Opstad
Borregaard, Postboks 162, 1701 Sarpsborg, Norway

E. B. Heggset · K. Syverud (✉)
RISE PFI, Høgskoleringen 6b, 7491 Trondheim, Norway
e-mail: kristin.syverud@rise-pfi.no

Graphical abstract

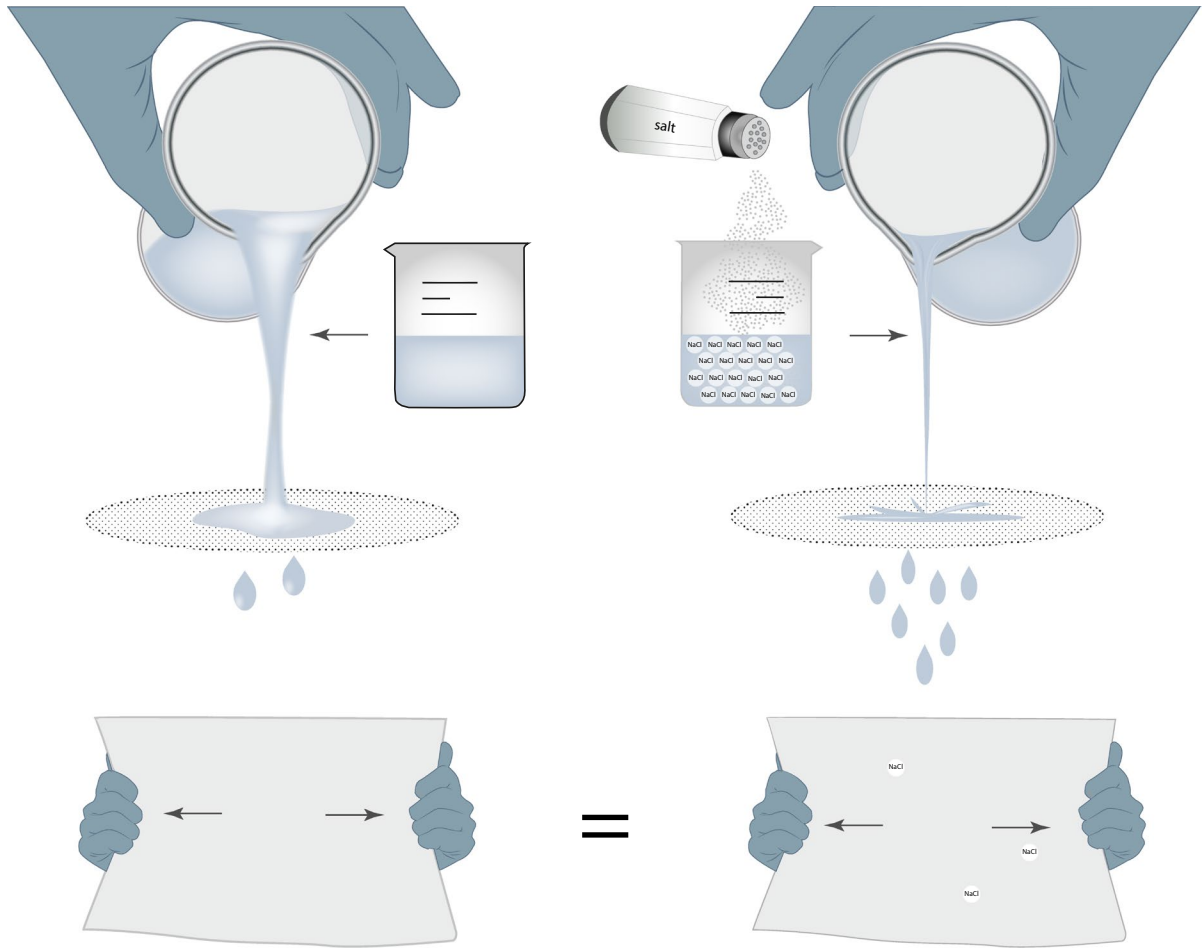

Keywords Nanocelluloses · Cellulose nanofibrils · Dewatering · Redispersion · Rheology

Introduction

Nanocelluloses comprise a group of cellulosic materials with dimensions in nanoscale that are hydrophilic, crystalline, stiff, and high aspect ratio fiber-like particles isolated from various natural sources. Their small width (2–100 nm) provides a very large specific surface area (30–200 m^2/g) (Spence et al. 2010). Often nanocelluloses are chemically modified to add functionalities by, for example, introducing ionizable groups (surface charges), which also facilitates isolation of the particles and provides good dispersibility and stability in water. The isolation of nanocellulose particles has allowed for bottom-up formation of many types of materials (e.g., films, foams and fibers) with fascinating properties such as strong and light, transparent and with great gas barrier (Dufrense 2012).

Because dispersions of nanocelluloses are highly viscous and shear thinning, different types of nanocelluloses have been studied as rheological modifiers (Herrick et al. 1983; Pääkkö et al. 2007; Karppinen et al. 2011; Dimic-Misic et al. 2017; Aaen et al. 2019a; Heggset et al. 2019). Additionally, as fibrillar

networks are formed at very low concentrations, nanocelluloses have been utilized to disperse several exotic materials in water media by trapping them in the network (Chu et al. 2020), e.g. carbon nanotubes (Hajan et al. 2017), graphenes (Yang et al. 2017) and metal organic frameworks MOFs (Zhu et al. 2016), as well as using them for co-fibrillation and high shear grinding of agglomerated particles into smaller, dispersed suspensions (Dimic-Misic et al. 2019).

However, nanocellulose suspensions are hard to dewater, providing tedious and costly drying procedures, which significantly limit the industrial use of nanocelluloses. This is especially true for cellulose nanofibrils (CNFs), which are the focus of this study. From the CNF producers' point of view, excessive amounts of water in CNF suspensions increase the shipment cost. Thus, concentrated suspensions are preferred for shipment which then can be redispersed with preserved properties by the receiver. It is claimed that the dewatering – drying process is a key barrier to successful commercialization (Sinquefield et al. 2020). CNCs can even be dried with good redispersibility if charged and dried with a metal counterion (Beck et al. 2012). However, most CNFs irreversibly aggregate during drying, causing loss in properties. Their higher aspect ratio leads to increased particle interactions/entanglements, rendering clustered suspensions upon redispersion.

The reasons that CNFs are hard to dewater are their high hydrophilicity, small dimensions which provides large specific surface area, and high aspect ratio (Hubbe et al. 2017). These properties generates kinetically arrested networks (gels) at low solid contents that holds water very strongly. The concentration of the network formation depends on many factors, for example fibrillation degree, aspect ratio and surface chemistry (Mendoza et al. 2018). These networks needs to be compressed to remove water but the network strength increases exponentially with the CNF concentration (Naderi et al. 2014; Aaen et al. 2019a), making it increasingly hard to dewater. Finally, the particles are often charged, increasing their hydrophilicity and providing an osmotic driving force holding/absorbing water (Aaen et al. 2019b). All these factors provide a very high water-holding capacity and network strength, making it highly energy demanding and time consuming to dewater CNF suspensions.

Vacuum filtration is used in papermaking and applied in academia to dewater CNF suspensions. However, the process is too slow, taking hours for fine qualities of CNFs. In addition, the concentration reached by vacuum dewatering is relatively low, 5–10 wt%. In papermaking wet pressing is often used for dewatering pulp. Its energy efficiency and rapidness (Unbehend and Britt 1982) are intriguing, however, the dewatering time by pressing is substantially increased if CNFs are added to pulp (Rantanen and Maloney 2015). It has been shown hard to press pure CNF suspensions. Instead of dewatering, the pressing often breaks the CNF gels in fragments or squeezes out the CNF suspension from the press geometry. By using a confined pressing configuration Wetterling et al. (2017) was able to dewater suspensions of the larger sized non-charged microcrystalline cellulose (MCC) particles, and later suspensions of charged cellulose nanocrystals (CNCs) (Wetterling et al. 2018). A constant mechanical pressure of 3 bars was used and the effect of the chemical environment (ionic strength and pH) and the application of an electrical field were investigated. The dewatering of the pure MCC suspension was slow (0.2–1 mL/min, faster in the beginning, slower towards the end), but changing the environment or applying an electrical field increased the rate by more than an order of magnitude. Combining the two further increased the rate, but at the cost of a higher energy demand. The addition of ions resulted in a higher voltage for the same electrical field. The dewatering of CNC suspensions was facilitated in a similar manner. Similar trends are expected for CNF suspensions.

Dimic-Misic et al. (2013a) combined rheology measurements with vacuum filtering to better understand why CNF suspensions are so slow to dewater. High and low charged CNFs were compared. The former was substantially slower, even though the rheological properties (viscosity and storage modulus) were lower and less affected by the dewatering. The higher homogeneity in combination with the smaller size of the finer CNFs was suggested to be the prime reason for these effects. In another study by Dimic-Misic et al. (2013b), oscillatory and rotational shear was altered during dewatering of furnishes including nanocellulose. It was argued that this altering may induce a restructuring of the particles favoring dewatering. These new insights are intriguing. Still, more knowledge is needed on how dewatering can be facilitated by chemical and structural changes without hampering decisive properties of the final material.

Table 1 CNF suspensions with alternation of salt concentration and pH. Enz = enzymatically pretreated CNFs, Carb = carboxymethylated CNFs, Ind = industrial quality, i.e., Exilva from Borregaard

CNF system	Kind of CNF	Added NaCl (mM)	pH adjustment	Conductivity (μS/cm)
Enz CNF	Enzymatically pretreated	0	No (pH 7)	41
Enz CNF 10 mM NaCl	Enzymatically pretreated	10	No (pH 7)	1501
Enz CNF 100 mM NaCl	Enzymatically pretreated	100	No (pH 7)	6910
Enz CNF pH 3	Enzymatically pretreated	0	Adj to 3	714
Enz CNF pH 5	Enzymatically pretreated	0	Adj to 5	84
Carb CNF	Carboxymethylated	0	No (pH 7)	272
Carb CNF 10 mM NaCl	Carboxymethylated	10	No (pH 7)	1580
Carb CNF 100 mM NaCl	Carboxymethylated	100	No (pH 7)	7000
Carb CNF pH 3	Carboxymethylated	0	Adj to 3	1277
Carb CNF pH 5	Carboxymethylated	0	Adj to 5	599
Ind CNF	Industrial	0	No (pH 5)	39
Ind CNF 10 mM NaCl	Industrial	10	No (pH 5)	1547
Ind CNF pH 3	Industrial	0	Adj to 3	854

Coagulation or flocculation are common techniques to obtain separation of solids and liquid water in e.g. water treatment of sludge. Suspended material is destabilized by diminishing their surface charge by adding coagulants of opposite charge. The destabilized particles aggregate and settle down (Wei et al. 2018). In water treatment of sludge, dispersibility is not an issue. However, additives have been shown to improve redispersibility in CNF samples, for example: NaCl (Missoum et al. 2012), glycols (Schnell and Jensen 2007), and polysaccharides (Häggblom and Vuorenpalo 2014; Beaumont et al. 2017). But these additives are often unwanted in the final products and, thus, an extra cleaning step is needed for its use. Hence, concentrated pure suspensions are the current preferred alternative for shipment and storage. However, if they are concentrated too much the redispersibility is reduced. Ding et al. (2019) studied redispersibilty of both CNC and CNF suspensions as a function of solid content (up to 65 wt%). The CNFs were TEMPO oxidized which is similar to the carboxymethylated CNFs in our study. Reduced redispersibility was found for all samples concentrated above 20 wt%, which was argued to be due to hornification. From AFM images they saw a clear increase in particle size with increasing solid content. This was confirmed by a correlating reduction in accessible hydroxyl groups assessed by using fluorescent labeling of the nanocelluloses.

In this study we have investigated the dewatering of CNF suspensions from 1 wt% to about 20–30 wt%. Three different qualities were investigated: enzymatic pre-treated, an industrial grade, and carboxymethylated CNF, varying in charge, from low to high. The chemical environment was changed by adding different levels of salt (NaCl) or acid (HCl). The main objective has been to study the dewatering rate and correlating it to the suspension properties of the different samples. To assess whether the dewatering reduced the quality of the CNF dispersions, CNF films were prepared from the CNFs both before and after dewatering and redispersion. Their mechanical properties as well as oxygen permeability were assessed and compared. The aim of the study was to facilitate dewatering without hampering suspension and material properties of the different CNF qualities.

Materials and methods

The laboratory grade CNFs were prepared by fibrillation of a softwood sulphite dissolving pulp (Domsjö Dissolving plus, Domsjö Fabriker, Sweden). The hemicellulose content of the pulp was in previous study determined to be 4.5% (Naderi and Lindström 2016). Two different pretreatments were applied to the pulp prior to fibrillation; enzymatically pretreatment (Päkkäö et al. 2007; Henriksson et al. 2007) and carboxymethylation (Wågberg et al. 2008) with

modifications described by Naderi et al. (2016). Enzymatically (Enz) pretreatment was done, using 2.5 L phosphate buffer (pH = 7). To produce the Enz CNF the treated pulp was microfluidized (M-110EH, Microfluidics Corp., USA) at 2%, passed one time at 1700 bar through two Z shaped chambers in series with diameters of 200 and 100 µm. The charge of Enz CNF produced from this pulp was 30 µmol/g (Naderi and Lindström 2016). The carboxymethylated (Carb) pulp was microfluidized as the Enz CNF. The charge of Carb CNF was 604 µmol/g, determined by conductimetric titration on the pulp. The hemicellulose content of the raw material (see sulphite pulp above) is not expected to change by the production of the CNFs, hence the hemicellulose content is assumed to be 4.5%. The industrial grade CNF (Ind CNF) was Exilva, a mainly mechanically fibrillated CNF, provided by Borregaard, Norway. It was delivered at 10 wt% solid content and dispersed using deionized water to 2 wt% solid content according to instructions from the manufacturer. The charge was 106 µmol/g (Heggset et al. 2018) and the hemicellulose content 4.5% (assessed by manufacturer).

Analytical grades of NaCl and HCl were purchased from VWR.

Alteration of salt concentration and pH

The original 2 wt% CNF suspensions were diluted with deionized water to 1 wt%. For the samples with adjusted chemical environment salt or acid was added in this step using 1 M NaCl or 1 M HCl solutions, respectively. After dilution/adjustments all samples were passed once again through the microfluidizer at 400 bars. Overview of the CNF suspensions is given in Table 1.

The pH of the pure suspensions was 7 for Carb and Enz CNF and pH 5.3 for Ind CNF.

The conductivity was measured on the 1 wt% suspensions before and after dewatering and redispersion, using 50 mL of dispersion and the instrument inoLab Cond Level 2 (WTW GmbH, Germany). Conductivity of the redispersions is presented in supplementary information (Table SI1).

Dewatering

A piston-press with filter paper (Munktell 00 H) was used for the dewatering. 91 g of the CNF dispersions with 1 wt% dry content was used per test. The dewatering was carried out according to the following pressure profile: 0.5 bar for 30 min, 1 bar for 30 min, 2 bar for 30 min, 4 bar for 30 min, and 6 bar for 30 min. The stepwise pressure increase was to avoid squeezing out the CNF suspensions from the press geometry. Due to low dewatering rate of the original Carb CNF suspension, Carb CNF 10 mM NaCl and Carb CNF adjusted to pH 5 the highest pressure of 6 bars was kept for 15–17 h (overnight) in order to reach equilibrium. The mass of the released water (filtrate) as function of time was recorded continuously using a balance. The dewatering rate was calculated as the slope between 10 and 30% mass loss. Each experiment was run in triplicate. The final weight of the filter cakes was used to calculate the final dry content. The curves presented are the average of the three batches for each CNF system.

Re-dispersion

The dewatered CNF filter cakes, 3 for each sample type, were immersed in water over night. After immersion the samples were propeller mixed for 2 min at 2000 rpm and thereafter mixed with Polytron for 30 s at 20 000 rpm. The final CNF concentration was 1 wt%.

Structure characterization

The samples were characterized using Atomic Force Microscopy (AFM), ultraviolet–visible (UV–Vis) spectroscopy.

AFM

The microscopic features of the samples were studied by AFM, using a Bruker Multimode V AFM equipped with a Nanoscope V Controller (Veeco Instruments Inc., Santa Barbara, CA, USA). The instrument was located at the NorFab facility NTNU Nanolab in Trondheim, Norway. When analyzing the suspensions, 25 µL of the solution (concentration of 0.1 wt%) was placed on freshly cleaved 10 mm mica (Agar Scientific Ltd., Essex, UK), and dried using compressed nitrogen gas (N_2) before imaging. Images were obtained by ScanAsyst mode in air at ambient conditions, with silicon nitride ScanAsyst-air AFM tips (Nom. Spring constant = 0.4 N m^{-1}, resonance frequency = 70 kHz), Bruker AFM Probes (Bruker Nano Inc., Camarillo, CA, USA). The surface

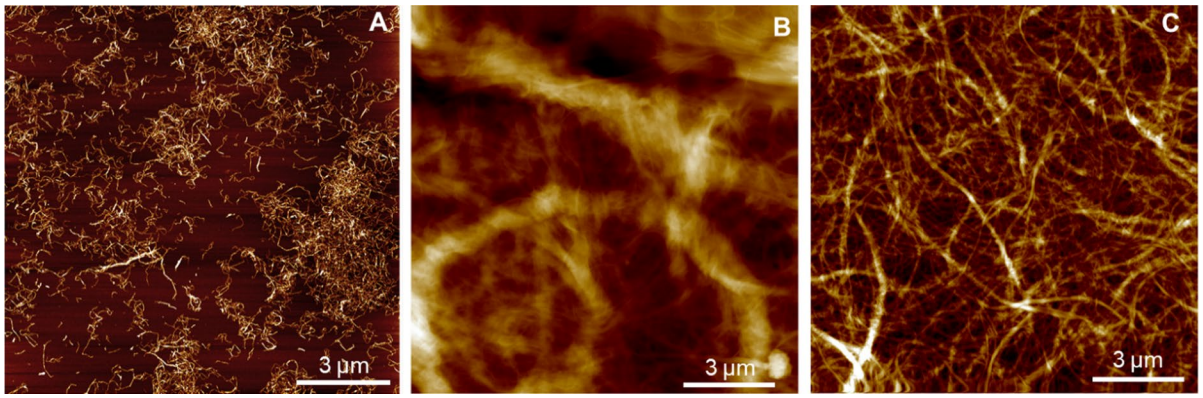

Fig. 1 AFM height images for Carb CNF (**A**), Enz CNF (**B**), and Ind CNF (**C**)

roughness was calculated using the NanoScopeAnalysis software, version 1.5.

Ultraviolet–visible (UV–Vis) spectroscopy.

The change in transmittance for the CNF dispersions before and after dewatering and redispersion was studied using a UV–Vis Spectrophotometer (UV-1800, Shimadzu, Tokyo, Japan). The samples were diluted to a concentration of 0.08 wt% and mixed properly using a IKA T18 Digital Ultra-Turrax at 4200 rpm for 7 min. Subsequently, the transmittance was measured at a wavelength of 500 nm using a cell path length of 1 cm and a slit width of 2.0 nm. Four parallels were measured for each sample.

Rheology measurements

Rotational shear ramp measurements were performed on 1 wt% CNF suspensions using a Kinexus stress-controlled rotational rheometer (Malvern Instruments, Malvern, UK) with a serrated bob and cup geometry. A previously reported protocol (Naderi et al. 2016) was followed with an integration time between measuring points of 30 s. The viscosity at the shear rate of 1 s^{-1} was collected from the ramps and used for comparison between samples.

Preparation and evaluation of CNF films

Vacuum filtrated films were prepared, tensile strength and oxygen permeability were evaluated following previously reported protocols (Naderi et al. 2016). The measurements were conducted at 23 °C and 50% RH.

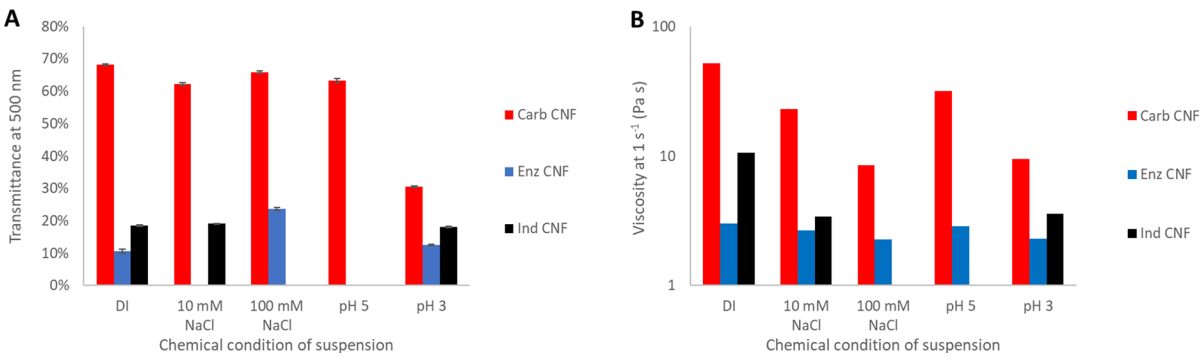

Fig. 2 In A is the transmittance of 0.08% dispersions shown. B shows the transient viscosity at 1 s^{-1} taken from the shear ramp measurements of 1% CNF dispersions with and without NaCl additions or pH adjustments

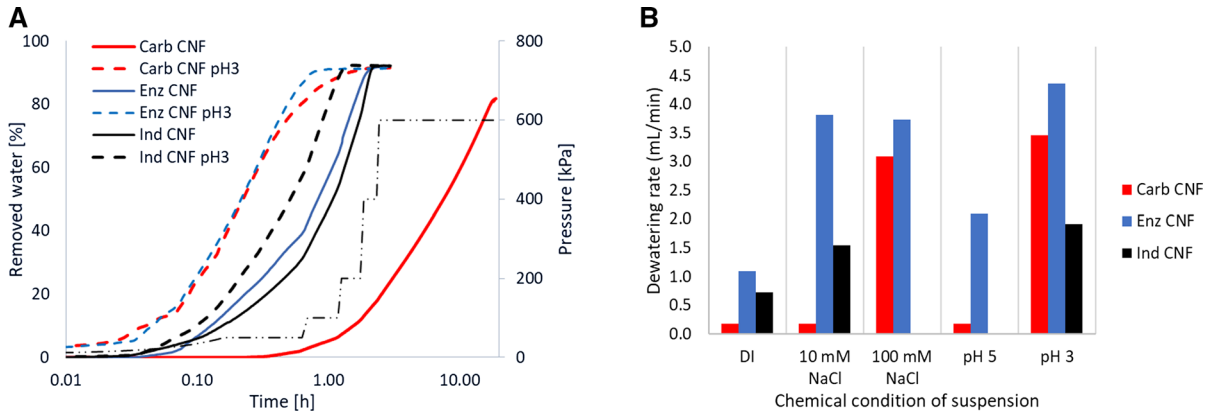

Fig. 3 Removed water as a function of dewatering time for the pure CNF suspensions and at pH 3 (**A**). Dewatering rate for the different CNF qualities at the different chemical conditions (**B**). The dewatering rate is calculated as the slope between 10 and 30% removed water

Results and discussion

Suspension properties and particle structure

AFM images of the different CNFs are shown in Fig. 1 and transmittance and viscosity in Fig. 2. The three types of CNFs are clearly different. Carb CNF is the most fibrillated showing a finer structure in the AFM image (Fig. 1A) and higher transmittance, and viscosity (Fig. 2). The AFM image of Enz CNF (Fig. 1B) shows coarsest structure. It has also the lowest transmittance and viscosity (Fig. 2A, B) of all the three CNFs, indicating the lowest degree of fibrillation. The AFM image of Ind CNF (Fig. 1C) show finer and more homogenous particle structure than Enz CNF, but still clearly larger structures than for Carb CNF (Fig. 1 A). Similarly, its transmittance and viscosity are in between the other two CNF qualities (Fig. 2A and B). Hence the properties correlated with surface charge of the CNFs. The effect of changing the chemical environment, i.e. reducing the electrostatic repulsion, was investigated by adding salt or acid. The properties of the lowest charged CNF (Enz) do not change much by the additions. The viscosity and the transmittance are only slightly affected (Fig. 2 A and B, blue bars). For the slightly higher charged Ind CNF (106 compared to 30 µmol/g) the alterations mainly have an effect on the viscosity (Fig. 2D, black bars). However, the transmittance stays unaffected indicating that aggregation is negligible (Fig. 2B). The largest effect, as expected, is observed for the high charge Carb CNF (604 µmol/g). Both addition of salt and acid to the Carb CNF suspensions reduce the viscosity (Fig. 2B, red bars), with largest reduction at 100 mM NaCl and pH 3, while the transmittance reduces the most at pH 3 (Fig. 2 A). This indicates aggregation of Carb CNF especially at pH 3.

Dewatering

In the dewatering experiments, the different CNF suspensions were dewatered in the piston press device with stepwise increased pressure from 0.5 to 6 bar (Fig. 3A). The pure suspensions release water very differently (Fig. 3A, solid lines). Dewatering of Carb CNF is substantially slower than that of the two lower charged CNFs (Enz and Ind CNF). The Carb CNF has not reached equilibrium even after 19 h of dewatering whereas equilibrium is reached after approximately 2 h for the others. An explanation of the slow dewatering suggested in the literature is formation of a dense, strong homogenous gel of fine fibrillar structure (Dimic-Misic et al. 2013b). In addition, the high charge of the material makes it more hydrophilic and osmotically prone to swell and hold water. The dewatering rate follows the order Enz CNF > Ind CNF > Carb CNF. This is in accordance with what to be expected from the order of the charge of the samples, Enz CNF < Ind CNF < Carb CNF, and the degree of fibrillation, that follows the same order (Fig. 1).

The effects on the dewatering rate after altering pH or adding NaCl are shown in Fig. 3A (dotted lines) and the results for all the samples are summarized in Fig. 3B. Changing the chemical environment can have a substantial effect on the dewatering rate, especially when largely changed. At pH 3 all three types of CNFs dewater considerably faster, as well as at 100 mM NaCl for Carb and Enz CNF (not measured for Ind CNF). Under these conditions the electrostatic effects are to a large extent cancelled out. The surface charge is almost completely turned off at pH 3 (Fall et al. 2011), as pKa of carboxylic groups attached to cellulose are around 4.8 (Lindgren and Öhman 2000. Thus, when turning off the charges, higher charged Carb CNF start to behave as the lower charged Enz and Ind CNF. Actually, the raw material and production process may be more important at pH 3 as Enz and Carb CNF, that are produced by the same mechanical treatment and using the same pulp, behaves more similarly, than Ind CNF that is produced from a different pulp and using a different mechanical treatment. In addition, at pH 3 Carb CNF is expected to aggregate (Fall et al. 2011), however, in this study the dispersions are homogenized after the pH adjustment (NaCl addition) so aggregation may be reduced. Larger aggregated structures would increase the distance between structures, creating channels for water transport and thus increasing the dewatering rate. One should also bear in mind that adjusting the pH will increase the ionic strength. By assuming that all charged groups are protonated at pH 3, the ionic strength will be 7 mM for Carb CNF and 2 mM for Ind CNF and 1.3 for Enz CNF. That the three CNFs have different ionic strength at pH 3 is verified by the conductivity of the dispersions (Table 1), arranged in the order of the surface charge. As the dewatering is affected more at pH 3 than at 10 mM and even at 100 mM NaCl, it is suggested that the major effect is the pH effect and not the increase in ionic strength. The dewatering rates are similar for Enz CNF and Carb CNF at 100 mM NaCl. This could be because most charge interactions are canceled out at this ionic strength, providing very low electrostatic repulsion between particles, i.e. low surface potentials (Fall et al. 2011). Reducing the influence of charge, makes Carb CNF and Enz CNF similar as in the case of pH 3. For lower charged particles as the Enz and Ind CNF the electrostatic repulsion is expected to be significantly reduced already at 10 mM NaCl, whereas the repulsion is still significant for Carb CNF, explaining why faster dewatering rates are obtain already at the lower NaCl level for the two lower charged CNF qualities. The effect is the largest for the lowest charge Enz CNF, close to the fastest dewatering rate, which occur at pH 3 for all CNFs. The slightly more charged Ind CNF may still be electrostatically active at 10 mM NaCl but not at pH 3, explaining its further increase in dewatering rate at pH 3. For the pH adjustment the same trend is observed, an increase in dewatering rate already at pH 5 is observed for Enz CNF whereas Carb CNF stays unaffected (not measured for Ind CNF). However, the dewatering rate of Enz CNF continues to increase with further adjusting the pH to 3. Once again at pH 5 the electrostatic interactions are expected to be significantly reduced for Enz CNF whereas they are barely affected for Carb CNF (Fall et al. 2011). Still the repulsion of Enz CNF is expected to be larger at pH 5 compared to at 10 mM NaCl (Fall et al. 2011), supporting the lower dewatering rate at pH 5.

The addition of salt and acid will also reduce osmotic driven counter force for releasing water from the CNF suspensions. If the ion concentration of the released water is significantly lower than the ion concentration of the CNF suspension, which includes both the added ions and the counterions to the charges, an osmotic force will be generated to hold the water within CNF network. Note that the counterions associated to CNFs surface charges will not be released during the dewatering. For the original suspensions pure water will be released and the strongest osmotic force will be generated, which will be stronger with increased surface charge, as it provides more counterions. The counterion concentration at 1 wt% for Carb CNF is about 6 mM, for Ind CNF 1 mM and for the Enz CNF around 0.3 mM, providing an ionic strength of half of these values (3, 0.5 and 0.15 mM). If the added salt concentration is significantly higher than the native ionic strength of the dispersions the osmotic force will be negligible. However, note that this osmotic force will increase as the sample is dewatered since the counterions will not be released. In addition, reducing pH will protonate the carboxylic charges and, thus, release the counterions, further reducing the osmotic force. As the dewatering rate of Enz CNF is significantly increased at 10 mM NaCl and at pH 5, where the viscosity is barely affected, the reduction in the osmotic force

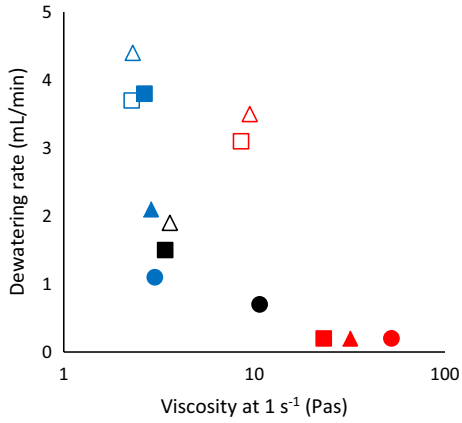

Fig. 4 The relation between transient viscosity and dewatering rate. Red marks show Carb CNF, blue Enz CNF and black Ind CNF. Filled circles reflect the original suspensions. Squares illustrate NaCl additions (filled 10mM and open 100mM), and triangles illustrate pH adjustments (filled pH 5 and open pH 3)

Table 2 Dry content at the end of dewatering (starting dry content 1 wt%)

CNF system	Final dry content (% (w/w))
Enz CNF	28
Enz CNF 10 mM NaCl	23
Enz CNF 100 mM NaCl	21
Enz CNF pH 3	23
Enz CNF pH 5	32
Carb CNF	15*
Carb CNF 10 mM NaCl	17*
Carb CNF 100 mM NaCl	16
Carb CNF pH 3	21
Carb CNF pH 5	17*
Ind CNF	33
Ind CNF 10 mM NaCl	30
Ind CNF pH 3	25

*Kept at 6 bar for 15–17 h (overnight)

may be an important factor. For Ind CNF the osmotic force is also highly reduced at 10 mM as this is higher than the concentration of the counterions, supporting the faster dewatering rate. For Carb CNF the higher charge provides lower reduction in the osmotic force at low additions of salt and acid. At 10 mM NaCl the osmotic force is still present. The removed water will have an ionic strength of 10 mM whereas the ionic strength of the CNF dispersion is initially 13 mM, resulting in an osmotic water holding force that will increase in strength as the system dewaters. At 100 mM NaCl the osmotic force is largely reduced for Carb CNF as well, which may increase its dewatering rate, 100 mM of the released water compared to 103 of the dispersion at the initial state. At pH 3 the osmotic force is cancelled out as the charges are protonated, which supports why the dewatering rate is faster at pH 3 compared to at 100 mM NaCl.

As the osmotic force is hard to measure or estimate, the parameter that shows the best correlation with the dewatering rate in our study is the viscosity, i.e. faster dewatering with lower viscosity (Fig. 4). It appears to be a threshold in viscosity, above no effect is found but below it has a large impact. This threshold may be related to the specific dewatering setup and procedure used in the study. The figure shows that the coarser qualities of this study, Enz and Ind CNF, follow a similar pattern whereas the more fibrillated Carb CNF has its own pattern. This is reasonable as Carb CNF differs, both chemically and structurally, from the two other CNFs.

When salt and acid are added, the viscosity drops, and faster dewatering is observed (Fig. 4). However, many other properties of the suspensions will be affected as well, some that might be decisive for rapid dewatering. Dewatering is a complicated phenomenon. It is affected by the hydraulic permeability and the viscoelasticity of the particle network (Hubbe and Heitmann 2007). The viscosity before dewatering describes indirectly how fine the fibrillar structure is. It has been shown that if the fine particles are fractionated out from a CNF suspension, by filtration followed by centrifugation, this fraction provides an almost 10-fold increase in rheological properties, when measured and compared at same solid content as the original non-fractionated suspension (Larsson et al. 2019; Ciftci et al. 2020). The studies used similar CNFs to the Ind CNF in our study. Our results also show significantly higher viscosity for the finer Carb CNF. The suspension's permeability is crucial for how fast it dewaters. The structure of fine material is strongly related to the systems permeability (finer structures, lower permeability), which probably is an important factor for the strong correlation between the viscosity and the dewatering rate.

The final dry content is shown in Table 2. The levels are mostly between 20 and 30%. According

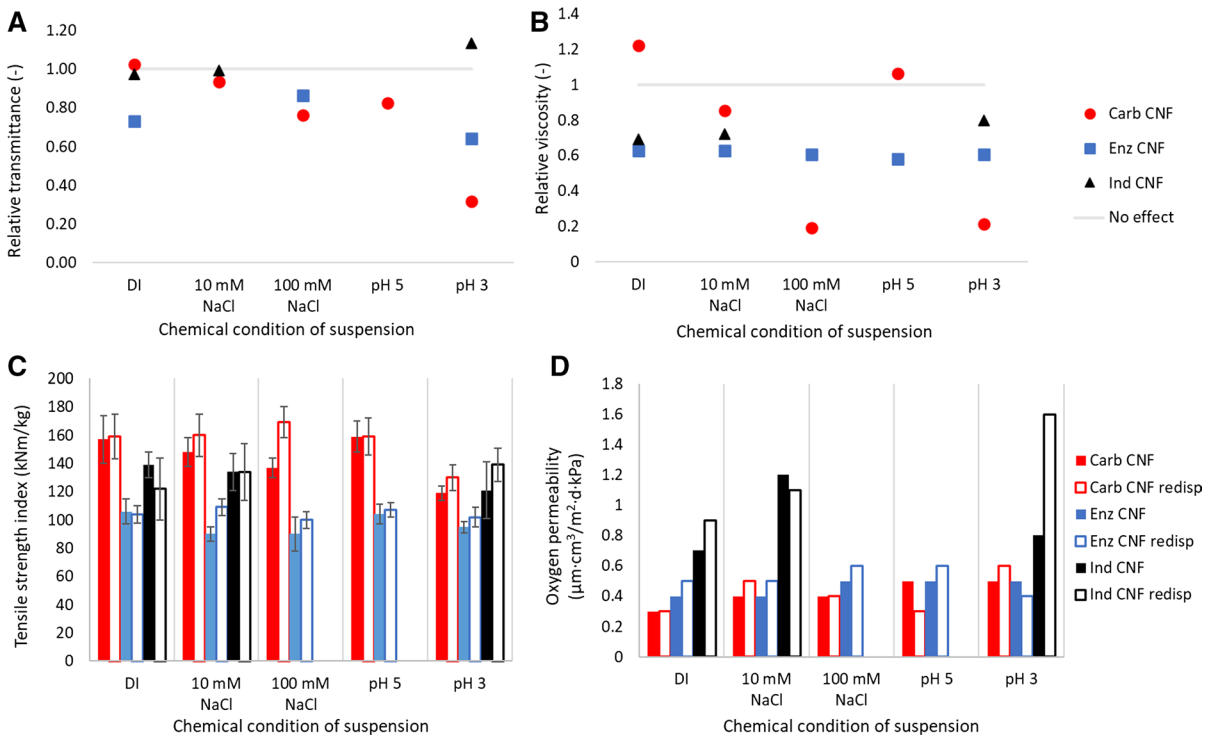

Fig. 5 Relative changes in transmittance (**A**) and viscosity (**B**) after dewatering and redispersion. Tensile strength index (**C**) and oxygen permeability (**D**) for films prepared with the different CNF systems before and after dewatering and redispersion

to Sinquefield et al. (2020), removing free water will give a sold content of about 30%, meaning that it is free water that is removed. It seems easier to remove larger amount of water from the coarser CNF qualities Enz and Ind compared to the finer Carb CNF, as they reach a higher final dry content. The larger particle structures of Enz and Ind CNF compared to Carb CNF are expected to generate networks of higher hydraulic permeability, potentially explaining their higher final solid content. Enz CNF, generally, reaches a lower final solid content than Ind CNF. This may be explained by its more heterogeneous structure size indicated by the AFM image (Fig. 1). The smaller particles may penetrate the network structure generated by the larger particles and plug channels. Similarly, in papermaking smaller fines can plug the channels created by larger pulp fibers (Hubbe and Heitmann 2007). When salt and acid is added, a lower final solid content is reached for the coarser CNF qualities, but a higher for Carb CNF, especially at pH 3. The additions will cause the particle–particle interactions to go from repulsive to more and more attractive and eventually cause particle aggregation (Fall et al. 2011), but it may also create stronger fibrillar networks (Saito et al. 2011) if the aggregation is limited. As we in this study homogenize the suspensions after the salt/acid additions, increased structure size by aggregation is promoted. The large drop in transmittance and viscosity for Carb CNF indicates formation of larger structures. This provides fewer contacts between aggregated CNFs and is expected to reduce the network strength. For the other two CNFs the structure size is less effected and the stronger particle–particle interactions may instead create stronger particle networks. This would potentially explain why the additions provide reduction in solid content for these two CNFs.

To conclude, altering the chemical environment is very powerful for increasing the dewatering rate, but it comes with a cost of lower final dry content for the coarser CNFs whereas for Carb CNF both the rate and the final dry content is increased.

Effect of dewatering on suspension properties

Figure 5 A, B show the relative change in the suspension properties transmittance and viscosity after dewatering and redispersion compared to the properties of the original dispersions. The relative values are calculated by normalizing the values with the properties of the original suspensions before dewatering. The three different CNFs are affected differently. Carb CNF is the most sensitive. However, at neutral conditions it redisperse very well, and the relative properties are close to 1. The redispersion is also good at the colloidal stable conditions (10 mM NaCl and pH 5), with only marginal reduction in the relative properties. However, once Carb CNF aggregates (100 mM NaCl and pH 3) the relative properties are significantly reduced, especially for pH 3. In the case of 100 mM NaCl, the drop is less pronounced for the relative transmittance. Comparing Enz CNF to Carb CNF, the original suspension of Enz CNF is more sensitive to dewatering, but no further reduction is seen by the addition of salt or acid. Changes in chemical environment also marginally affect the relative properties of Ind CNF, but it redisperses slightly better than Enz CNF. Besides the chemical condition of the suspensions, the final dry content may also affect the redispersibility. Ding et al. (2019) showed that above 20 wt% nanocellulose suspensions start to hornify, causing irreversible structure formation which reduces suspension redispersability. Enz and Ind CNF are generally dewatered to a higher final dry content than Carb CNF, which, by hornification may explain their poorer redispersibility. The lower relative transmittance of Carb CNF pH 3 versus Carb CNF 100 mM NaCl may also be explained by the higher solid content after dewatering at pH 3, 21 wt% and 16 wt%, respectively. The dewatering and redispersion reduces the NaCl concentration to about 5 mM, thus the Carb CNF is in colloidal stable state during the redispersion and de-aggregation can be expected. When the pH 3 dispersion is redispersed the counterion has been changed from sodium to hydrogen which may explain its poorer redispersion. In addition, the dispersion will be at pH 4 during the redispersion where the Carb CNF is expected to be less colloidally stable compared to at 5 mM NaCl.

Vacuum filtrated films were prepared from the different CNF systems before and after dewatering and redispersion and evaluated with respect to mechanical properties and oxygen barrier (Fig. 5C, D). In general, the mechanical properties are the best for Carb CNF followed by Ind CNF and then Enz CNF, hence higher charge and fibrillations seems to generate stronger films. Dewatering and redispersion has little effect on the mechanical properties for all original CNFs. The strength also stays rather unaffected by the addition of salt and acid. It is mainly Carb CNF at pH 3 that shows a clear effect on the film strength, reducing it by 20%. This was also observed by Benitez and Walther (2017), reporting a 50% reduction. At this pH all charges (carboxyls) are expected to be turned off by protonation. But for Ind and Enz CNF that has significantly lower charge, the pH reduction has limited effect on the film strength. The dewatering and redispersion, which removes parts of the added salt or acid, generate in most cases stronger films. This is especially the case for Carb CNF 100 mM NaCl. The NaCl concentration after redispersion is calculated to be approx. 5 mM. At this ionic strength Carb CNF is expected to be in a colloidal stable state during the film formation, which may explain the strength improvement. The effect is not as strong after redispersing the dewatered pH 3 Carb CNF dispersion. However, in this case the counter ion has been changed from Na^+ to H^+ and the sample also seems to be more aggregated, showing both a low relative transmittance and viscosity.

Regarding oxygen barrier, Carb CNF performs the best once again but here Enz CNF show better barrier than Ind CNF films (Fig. 5D). Perhaps a more energy intense fibrillation process of Enz CNF (verses Ind CNF) could generate a fraction of very small particles that is beneficial for forming compact films. For the dispersions before dewatering and redispersion, salt and acid additions affect Carb CNF the most, followed by Ind CNF, and Enz CNF the least. Hence, higher particle charge results in higher sensitivity of the chemical environment. Ind CNF seems to be more sensitive to the addition of salt whereas Carb CNF is slightly more affected by pH adjustments. Dewatering and redispersion generally results in slightly higher permeabilities, indicating that the hornification upon the concentration increase may be a factor, creating slightly larger particle structures that forms less compact films.

Conclusions

Dewatering of CNF suspensions was studied by using a piston press setup for three different types of CNFs, two coarser qualities, i.e. one enzymatic pretreated grade and one industrial grade (Enz CNF and Ind CNF), and one finer and highly charged grade, i.e. pretreated using carboxymethylation (Carb CNF). The charge density of the samples were 30, 106 and 604 µmol/g for Enz CNF, Ind CNF and Carb CNF, respectively, and the degree of fibrillation followed the same order. The dewatering rates were substantially increased by altering ionic strength and pH. The most drastic effect was observed when either 100 mM NaCl was added or when the pH was adjusted to 3. In both cases the time after which no more water was possible to press out of the gel dropped from 19 h to less than 1 h for Carb CNF. Under these conditions the Carb CNF releases water equally fast as the coarser CNFs, even though they also were substantially faster to dewater at these conditions. The viscosity before dewatering seemed to provide a good qualitative estimate of the dewatering rate, where lower viscosity gave faster dewatering. Different types of CNFs had different patterns when plotting dewatering rate against viscosity, but the general trend of increasing rate with decreasing viscosity was the same for all three CNFs. For the coarser CNF qualities (Enz and Ind) the dewatering stopped at a higher final dry content compared to Carb CNF (28 and 33 wt% compared with 15 wt%). Changing ionic strength or pH decreased the final dry content for the coarser CNFs whereas it increased for Carb CNF.

Suspension properties and properties of films prepared from the CNFs were evaluated after dewatering and redispersion. Enz CNF did not affect much by the additions of NaCl or adjustments in pH but was clearly affected by the dewatering, especially the viscosity reduced upon redispersion. Ind CNF was less affected, especially regarding the transmittance. Addition of NaCl affected the properties of Enz and Ind CNF more than the pH adjustments. Carb CNF was highly affected with reduction in both suspension and material properties, especially after adjusting to pH 3. This condition provided the fastest dewatering but the reduction in properties is unfortunate. However, the addition of 100 mM NaCl almost provides as fast water removal with much lower reduction in properties for Carb CNF, especially for films produced from redispersed suspensions. For the coarser lower charged Enz and Ind CNFs the fast-dewatering rate at pH 3 could be fully utilized as it only provided minor reduction in properties, actually better properties than when NaCl was added. To conclude, the dewatering of CNF suspensions can be drastically improved by adjusting the suspensions pH or ionic strength, and the adjustment can be made so that the effect on suspension and film properties are limited.

Acknowledgments Åsa Engström, Alice Landmér, Anne-Marie Runebjörk (RISE) are acknowledged for carrying out the laboratory work, Birgitte H. McDonagh (RISE PFI) for performing the AFM characterization, Eva Kvernes Rygg for assistance with the TOC figure and Tom Lindström for valuable discussions during the initiation of this study.

Author contributions AF, MH, EH and KS: Study conception and design, material preparation, data collection and analysis, writing and revision of the manuscript. AK and AO: Revision of the manuscript. All authors read and approved the final manuscript.

Funding Open access funding provided by RISE Research Institutes of Sweden. This work was a part of the project NanoVisc: "Development of high-performance viscosifiers and texture ingredients for industrial applications based on Cellulose Nanofibrils (CNF)" financed by the Research Council of Norway through the Nano2021 programme (Grant No. 245300), and the companies Borregaard, Mercer, and Stora Enso. Part of the work has also been funded through the project NanoPlasma: Nanofibril production using plasma (Grant No. 274975) and from RISE.

Declarations

Competing interests All the authors declare no conflicts of interest.

References

Aaen R, Simon S, Brodin FW, Syverud K (2019a) The potential of TEMPO-oxidized cellulose nanofibrils as rheology modifiers in food systems. Cellulose 26:5483–5496. https://doi.org/10.1007/s10570-019-02448-3

Aaen R, Brodin FW, Simon S, Heggset EB, Syverud K (2019b) Oil-in-water emulsions stabilized by cellulose nanofibrils--the effects of Ionic strength and pH. Nanomaterials 9:259–272. https://doi.org/10.3390/nano9020259

Beaumont M, Konig J, Opietnik M, Potthast A, Rosenau T (2017) Drying of a cellulose II gel: effect of physical modification and redispersibility in water. Cellulose 24:1199–1209. https://doi.org/10.1007/s10570-016-1166-9

Beck S, Bouchard J, Berry R (2012) Dispersibility in water of dried nanocrystalline cellulose. Biomacromolecules 13:1486–1494. https://doi.org/10.1021/bm300191k

Benitez AJ, Walther A (2017) Counterion size and nature control structural and mechanical response in cellulose nanofibril nanopapers. Biomacromolecules 18:1642–1653. https://doi.org/10.1021/acs.biomac.7b00263

Chu Y, Sun Y, Wu W, Xiao H (2020) Dispersion properties of nanocellulose: a review. Carbohydr Polym 250:116892. https://doi.org/10.1016/j.carbpol.2020.116892

Ciftci GC, Larsson PA, Riazanova AV, Øvrebø HH, Wågberg L, Berglund LA (2020) Tailoring of rheological properties and structural polydispersity effects in microfibrillated cellulose suspensions. Cellulose 27:9227–9241. https://doi.org/10.1007/s10570-020-03438-6

Dimic-Misic K, Puisto A, Gane P, Nieminen K, Alava M, Paltakari J, Maloney T (2013a) The role of MFC/NFC swelling in the rheological behavior and dewatering of high consistency furnishes. Cellulose 20:2847–2861. https://doi.org/10.1007/s10570-013-0076-3

Dimic-Misic K, Puisto A, Paltakari J, Alava M, Maloney T (2013b) The influence of shear on the dewatering of high consistency nanofibrillated cellulose furnishes. Cellulose 20:1853–1864. https://doi.org/10.1007/s10570-013-9964-9

Dimic-Misic K, Maloney T, Liu G, Gane P (2017) Micro nanofibrillated cellulose (MNFC) gel dewatering induced at ultralow-shear in presence of added colloidally-unstable particles. Cellulose 24:1463–1481. https://doi.org/10.1007/s10570-016-1181-x

Ding Q, Zwng J, Wang B, Tang D, Chen K, Gao W (2019) Effect of nanocellulose fiber hornification on water fraction characteristics and hydrogen accessibility during dehydration. Carbohydr Polym 207:44–51. https://doi.org/10.1016/j.carbpol.2018.11.075

Dufrense A (2012) Nanocellulose. From nature to high performance tailored materials. De Gruyter, Göttingen

Fall A, Lindström S, Sundman O, Ödberg L, Wågberg L (2011) Colloidal stability of aqueous nanofibrillated cellulose dispersions. Langmuir 27(18):11332–11338. https://doi.org/10.1021/la201947x

Häggblom M, Vuorenpalo VM (2014) Method for producing dewatered microfibrillated cellulose. Patent number WO 2014/096547

Hajan A, Lindström BS, Petterson T, Hamedi MM, Wågberg L (2017) Understanding the dispersive action of nanocellulose for carbon nanomaterials. Nano Lett 17:1439–1447. https://doi.org/10.1021/acs.nanolett.6b04405

Heggset EB, Strand BL, Sundby KW, Simon S, Chinga-Carrasco G, Syverud K (2019) Viscoelastic properties of nanocellulose based inks for 3D printing and mechanical properties of CNF/alginate biocomposite gels. Cellulose 26:581–595. https://doi.org/10.1007/s10570-018-2142-3

Henriksson M, Henriksson G, Berglund L, Lindström T (2007) An environmentally friendly method for enzyme-assisted preparation of microfibrillated cellulose (MFC) nanofibers. Eur Polym J 43:3434–3441. https://doi.org/10.1016/j.eurpolymj.2007.05.038

Herrick FW, Casebier RL, Hamilton JK, Sandberg KR (1983) Microfibrillated cellulose: morphology and accessibility. J Appl Polym Sci Appl Polym Symp 37:797–813

Hubbe MA, Heitmann JA (2007) Review of factors affecting the release of water from cellulosic fibers during paper manufacture. BioResources 2:500–533

Hubbe MA, Tayeb P, Joyce M, Tyagi P, Kehoe M, Dimic-Misic K, Pal L (2017) Rheology of nanocellulose-rich aqueous suspensions: a review. BioResources 12(4):9556–9661

Karppinen A, Vesterinen AH, Saarinen T, Pietikäinen P, Seppälä J (2011) Effect of cationic polymethacrylates on the rheology and flocculation of microfibrillated cellulose. Cellulose 18:1381–1390. https://doi.org/10.1007/s10570-011-9597-9

Larsson PA, Riazanova AV, Ciftci GC, Rojas R, Øvrebø HH, Wågberg L, Berglund LA (2019) Towards optimised size distribution in commercial microfibrillated cellulose: a fractionation approach. Cellulose 26:1565–1575. https://doi.org/10.1007/s10570-018-2214-4

Lindgren J, Öhman LO (2000) Characterization of acid/base properties for bleached softwood fibers as influenced by ionic salt medium. Nord Pulp Pap Res J 15:18–23. https://doi.org/10.3183/npprj-2000-15-01-p018-023

Mendoza L, Gunawardhana T, Batchelor W, Garnier G (2018) Effects of fibre dimension and charge density on nanocellulose gels. J Colloid Interface Sci 525:119–125

Missoum K, Bras J, Belgacem MN (2012) Water redispersible dried nanofibrillated cellulose by adding sodium chloride. Biomacromolecules 13(12):4118–4125. https://doi.org/10.1021/bm301378n

Naderi A, Lindström T (2016) A comparative study of the rheological properties of three different nanofibrillated cellulose systems. Nord Pulp Paper Res J 31:354–363. https://doi.org/10.3183/npprj-2016-31-03-p354-363

Naderi A, Lindström T, Sundström J (2014) Carboxymethylated nanofibrillated cellulose: rheological studies. Cellulose 21:1561–1571. https://doi.org/10.1007/s10570-014-0192-8

Naderi A, Lindström T, Sundström J, Flodberg G, Erlandsson J (2016) A comparative study of the properties of three nanofibrillated cellulose systems that have been produced at about the same energy consumption levels in the mechanical delamination step. Nord Pulp Paper Res J 31:364–371. https://doi.org/10.3183/npprj-2016-31-03-p364-371

Pääkkö M, Ankerfors M, Kosonen H, Nykänen A, Ahola S, Österberg M, Ruokolainen J, Laine J, Larsson PT, Ikkala O, Lindström T (2007) Enzymatic hydrolysis combined

with mechanical shearing and high-pressure homogenization for nanoscale cellulose fibrils and strong gels. Biomacromolecules 8:1934–1941. https://doi.org/10.1021/bm061215p

Rantanen J, Maloney TC (2015) Consolidation and dewatering of a microfibrillated cellulose fiber composite paper in wet pressing. Eur Polym J 68:585–591. https://doi.org/10.1016/j.eurpolymj.2015.03.045

Saito T, Uematsu T, Kimura S, Enomae T, Isogai A (2011) Self-aligned integration of native cellulose nanofibrils towards producing bulk materials. Soft Matter 7:8804–8809. https://doi.org/10.1039/C1SM06050C

Schnell U, Jensen P (2007) Determination of maximum freeze drying temperature for PEG-impregnated archaeological wood. Stud Conserv 52:50–58

Sinquefield S, Ciesielski PN, Li K, Gardner DJ, Ozcan S (2020) Nanocellulose dewatering and drying: current state and future perspectives. ACS Sustain Chem Eng 8(26):9601–9615

Spence KL, Venditti RA, Rojas OJ, Habibi Y, Pawlac JJ (2010) The effect of chemical composition on microfibrillar cellulose films from wood pulps: water interactions and physical properties for packaging applications. Cellulose 17:835–848. DOI https://doi.org/10.1007/s10570-010-9424-8

Unbehend JE, Britt KW (1982) Retention, drainage, and sheet consolidation. Ind Eng Chem Prod Res Dev 21:150–153. https://doi.org/10.1021/i300006a004

Wågberg L, Decher G, Norgren M, Lindström T, Ankerfors M, Axnäs K (2008) The build-Up of polyelectrolyte multilayers of microfibrillated cellulose and cationic polyelectrolytes. Langmuir 24:784–795. https://doi.org/10.1021/la702481v

Wei H, Gao B, Ren J, Li A, Yang H (2018) Coagulation/flocculation in dewatering of sludge: a review. Water Res 143:608–631

Wetterling JS, Mattson T, Theliander H (2017) The Influence of Ionic strength on the electroassisted filtration of microcrystalline cellulose. Ind Eng Chem Res 56:12789–12798. https://doi.org/10.1021/acs.iecr.7b03575

Wetterling J, Sahlin K, Mattsson T, Westman G, Theliander H (2018) Electroosmotic dewatering of cellulose nanocrystals. Cellulose 25:2321–2329. https://doi.org/10.1007/s10570-018-1733-3

Yang W, Zhang Y, Liu T, Huang R, Chai S, Chen F, Fu Q (2017) Completely green approach for the preparation of strong and highly conductive graphene composite film by using nanocellulose as dispersing agent and mechanical compression. ACS Sustain Chem Eng 5:9102–9113. https://doi.org/10.1021/acssuschemeng.7b02012

Zhu H, Yang X, Cranston ED, Zhu S (2016) Flexible and porous nanocellulose aerogels with high loadings of metal-organic framework particles for separations applications. Adv Mater 28:7652–7657. https://doi.org/10.1002/adma.201601351